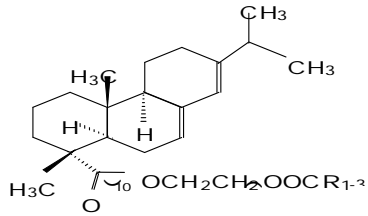
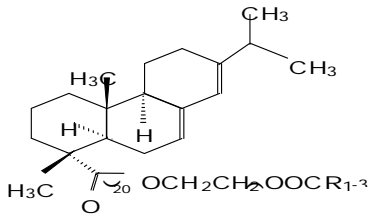
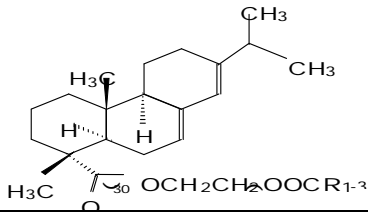
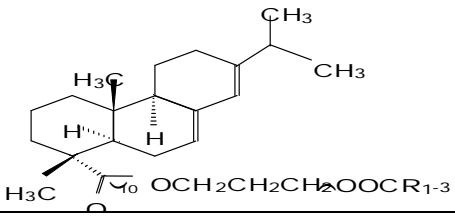
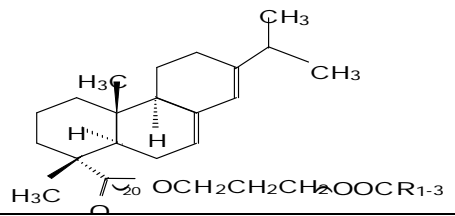
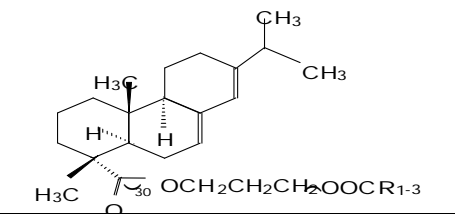


3.1 Chemical structures, names and abbreviations of prepared de-emulsifiers

In this work, 18 de-emulsifiers (surfactants) were prepared as described in the method section. The chemical structures and abbreviations of the prepared surfactants are listed in table 3.1.

Table 3.1 Chemical structure and abbreviation of the prepared de-emulsifiers

Chemical Structure	Name	Abbreviation
$R_{1-3}COO(CH_2CH_2O)_{10}H$	Ethoxylated Hydrolyzed Jatropa Oil (10 Unit)	HJ.E10
$R_{1-3}COO(CH_2CH_2O)_{20}H$	Ethoxylated Hydrolyzed Jatropa Oil (20 Unit)	HJ.E20
$R_{1-3}COO(CH_2CH_2O)_{30}H$	Ethoxylated Hydrolyzed Jatropa Oil (30 Unit)	HJ.E30
$R_{1-3}COO(CH_2CH_2CH_2O)_{10}H$	Propoxylated Hydrolyzed Jatropa Oil (10 Unit)	HJ.P10
$R_{1-3}COO(CH_2CH_2CH_2O)_{20}H$	Propoxylated Hydrolyzed Jatropa Oil (20 Unit)	HJ.P20
$R_{1-3}COO(CH_2CH_2CH_2O)_{30}H$	Propoxylated Hydrolyzed Jatropa Oil (30 Unit)	HJ.P30
$R_{1-3}COO(CH_2CH_2O)_{10}CO(CH_2)_7CH=CH(CH_2)_7CH_3$	Oleate Ethoxylated Hydrolyzed Jatropa Oil (10 Unit)	OHJ.E10
$R_{1-3}COO(CH_2CH_2O)_{20}CO(CH_2)_7CH=CH(CH_2)_7CH_3$	Oleate Ethoxylated Hydrolyzed Jatropa Oil (20 Unit)	OHJ.E20
$R_{1-3}COO(CH_2CH_2O)_{30}CO(CH_2)_7CH=CH(CH_2)_7CH_3$	Oleate Ethoxylated Hydrolyzed Jatropa Oil (30 Unit)	OHJ.E30
$R_{1-3}COO(CH_2CH_2CH_2O)_{10}CO(CH_2)_7CH=CH(CH_2)_7CH_3$	Oleate Propoxylated Hydrolyzed Jatropa Oil (10 Unit)	OHJ.P10
$R_{1-3}COO(CH_2CH_2CH_2O)_{20}CO(CH_2)_7CH=CH(CH_2)_7CH_3$	Oleate Propoxylated Hydrolyzed Jatropa Oil (20 Unit)	OHJ.P20
$R_{1-3}COO(CH_2CH_2CH_2O)_{30}CO(CH_2)_7CH=CH(CH_2)_7CH_3$	Oleate Propoxylated Hydrolyzed Jatropa Oil (30 Unit)	OHJ.P30

	<p>Rosin Ethoxylated Hydrolyzed Jatropa Oil (10 Unit)</p>	<p>RHJ.E10</p>
	<p>Rosin Ethoxylated Hydrolyzed Jatropa Oil (20 Unit)</p>	<p>RHJ.E20</p>
	<p>Rosin Ethoxylated Hydrolyzed Jatropa Oil (30 Unit)</p>	<p>RHJ.E30</p>
	<p>Rosin Propoxylated Hydrolyzed Jatropa Oil (10 Unit)</p>	<p>RHJ.P10</p>
	<p>Rosin Propoxylated Hydrolyzed Jatropa Oil (20 Unit)</p>	<p>RHJ.P20</p>
	<p>Rosin Propoxylated Hydrolyzed Jatropa Oil (30 Unit)</p>	<p>RHJ.P30</p>

3.2 FTIR Analysis

In order to prove the Jatropha oil hydrolysis, FTIR spectroscopy supported the FFA% by showing the main peaks and their corresponding functional groups. The comparison between Jatropha oil and its hydrolysis product are shown in figures 3.1 and 3.2.

Figure 3.1 showed the main difference between Jatropha oil and its hydrolysis product with complete disappearance of carboxylic acid carbonyl group, in the same time strong ester carbonyl group absorption band at 1746 cm^{-1} and 1164 cm^{-1} for stretching and bending vibrations respectively.

For carboxylic acid carbonyl functional groups (C=O), FTIR spectrum showed absorption bands of hydrolyzed oil at 1711 cm^{-1} for stretching vibration, $1283\text{-}1285\text{ cm}^{-1}$ for stretching asymmetric while at 1413 and 940 cm^{-1} for bending vibration of carboxylic acid. The hydrolyzed Jatropha oil IR showed ester carbonyl group absorption band at 1747 cm^{-1} and 1166 cm^{-1} indicates incomplete hydrolysis of Jatropha oil (figure 3.2).

Peaks at 2925 and 2855 cm^{-1} indicated the CH_2 and CH_3 stretching vibrations of both Jatropha oil and hydrolyzed oil. FTIR spectrum also showed absorption bands at 723 cm^{-1} for C-H group bending vibration. These results run in harmony with others (Salimon *et al.*, 2011).

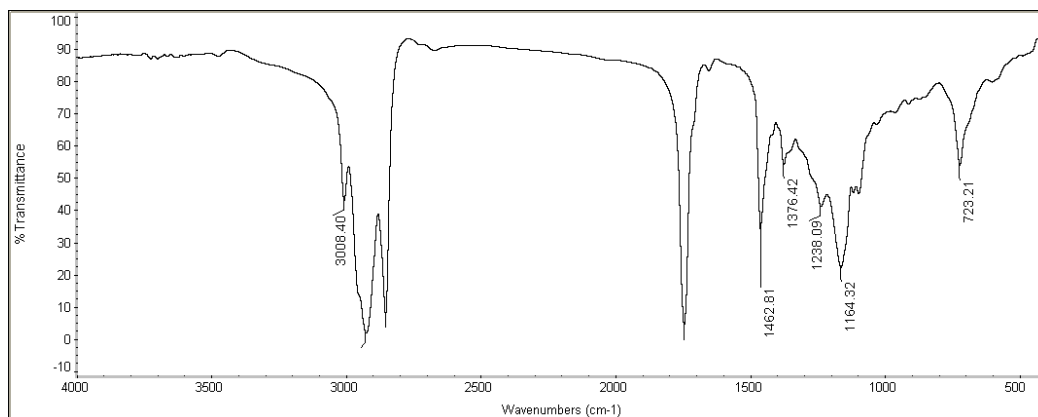


Fig. 3.1 FTIR spectrum of Jatropha oil

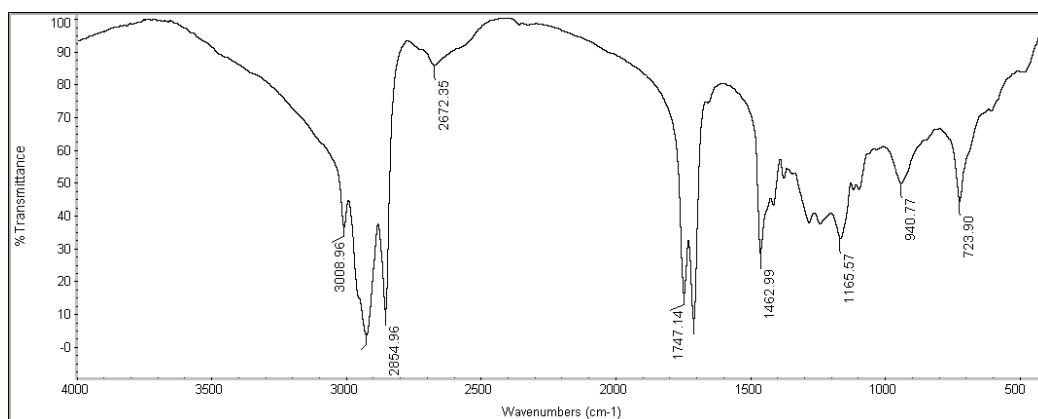


Fig. 3.2 FTIR spectrum of hydrolyzed Jatropha oil

Ethoxylated Jatropha fatty acids IR spectrum showed ester carbonyl group stretching vibration absorption band at 1736 cm^{-1} and bending vibration at 1125 cm^{-1} while at 2925 and 2855 cm^{-1} for CH_2 and CH_3 stretching vibration, C-H bending vibration showed absorption band at 723 cm^{-1} , and the absorption band at 1297 cm^{-1} for C-O stretching vibration, hydroxyl group showed stretching vibration absorption band at 3396 cm^{-1} and bending vibration absorption band at 1249 cm^{-1} (figure 3.3).

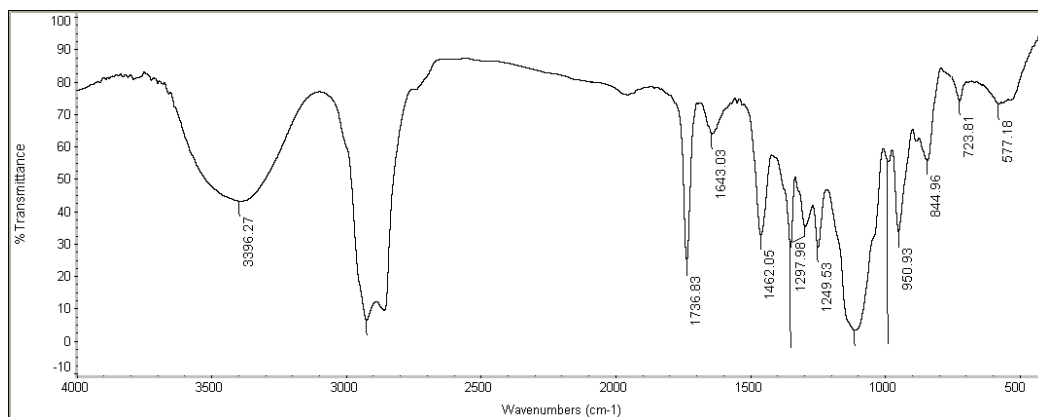


Fig. 3.3 FTIR spectrum of ethoxylated hydrolyzed Jatropha oil

Propoxylated hydrolyzed Jatropha oil IR spectrum showed weak ester carbonyl group stretching vibration absorption band –shoulder- at 1730 cm^{-1} and bending vibration at 1098 cm^{-1} while at 2929 and 2860 cm^{-1} for CH_2 and CH_3 stretching vibration, C-H bending vibration showed absorption band at 723 cm^{-1} , and the absorption band at 1297 cm^{-1} for C-O stretching vibration, the hydroxyl group showed stretching vibration absorption band at 3393 cm^{-1} (figure 3.4).

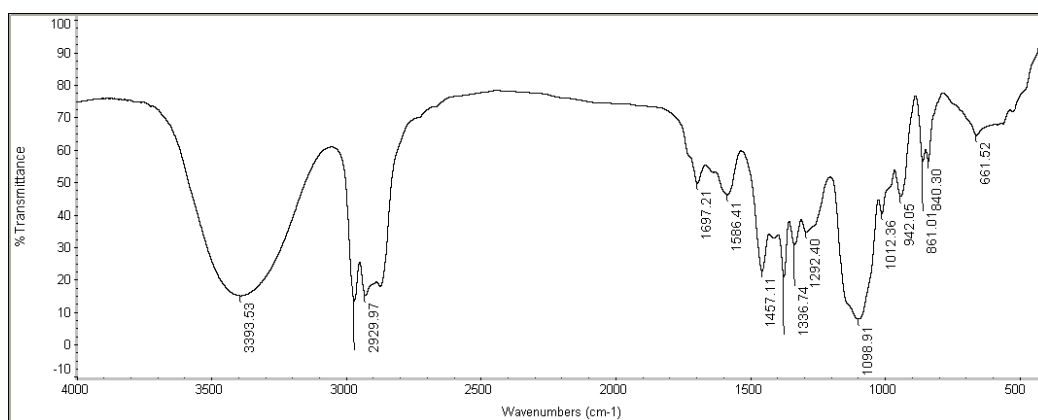


Fig. 3.4 FTIR spectrum of propoxylated hydrolyzed Jatropha oil

Oleate ethoxylated hydrolyzed Jatropha oil IR spectrum showed weak ester carbonyl group stretching vibration absorption band-shoulder- at 1725 cm^{-1} and bending vibration at 1100 cm^{-1} while at 2925 and 2855 cm^{-1} for CH_2 and CH_3 stretching vibration respectively, C-H bending vibration showed absorption band at 725 cm^{-1} , and the absorption band at 1298 cm^{-1} for C-O stretching vibration, carbon carbon double bond (C=C) showed stretching vibration absorption band at 1666 cm^{-1} (figure 3.5).

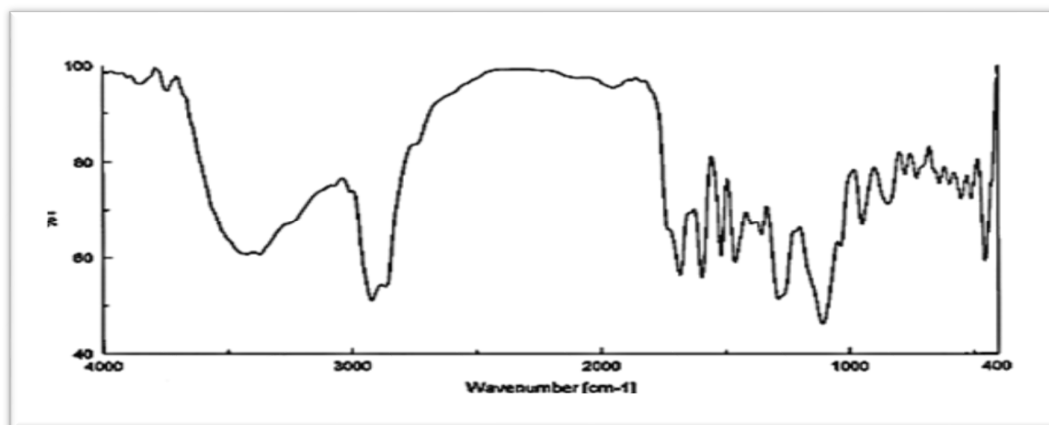


Fig. 3.5 FTIR spectrum of oleate ethoxylated hydrolyzed jatropha oil

Oleate propoxylated hydrolyzed Jatropha oil IR spectrum showed strong ester carbonyl group stretching vibration absorption band at 1735 cm^{-1} and bending vibration at 1125 cm^{-1} while at 2920 and 2850 cm^{-1} for CH_2 and CH_3 stretching vibration respectively, C-H bending vibration showed absorption band at 750 cm^{-1} , and the absorption band at 1280 cm^{-1} for C-O stretching vibration, carbon carbon double bond (C=C) showed stretching vibration absorption band at 1666 cm^{-1} (figure 3.6).

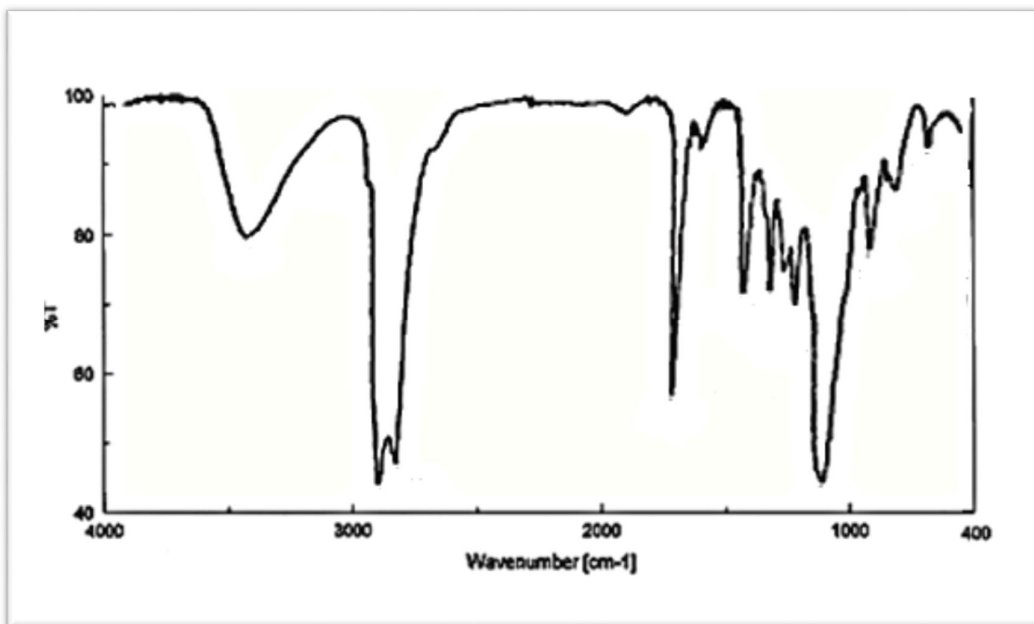


Fig. 3.6 FTIR spectrum of oleate propoxylated hydrolyzed jatropha oil

Rosin propoxylated hydrolyzed Jatropha oil IR spectrum showed strong ester C=O stretching vibration absorption band at 1730 cm^{-1} and bending vibration at 1050 cm^{-1} while at 2925 and 2855 cm^{-1} for CH_2 and CH_3 stretching vibration respectively, and bending at 750 cm^{-1} (figure 3.7).

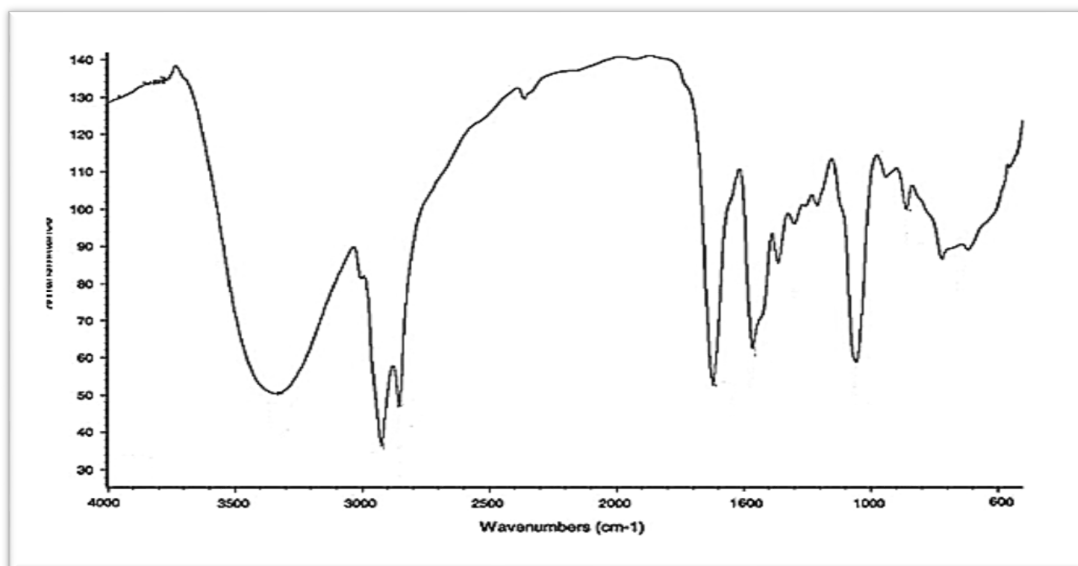


Fig. 3.7 FTIR spectrum of Rosin propoxylated hydrolyzed jatropha oil

3.3 Surface Tension Parameters

Micelles of de-emulsifiers are formed in bulk aqueous solution above a given concentration for each de-emulsifier and this concentration known as the critical micelle concentration (CMC). The CMC of the investigated individual surfactants (de-emulsifiers) at 60°C was determined by plotting the surface tension (γ) versus the logarithm of the de-emulsifier concentration ($-\ln C$).

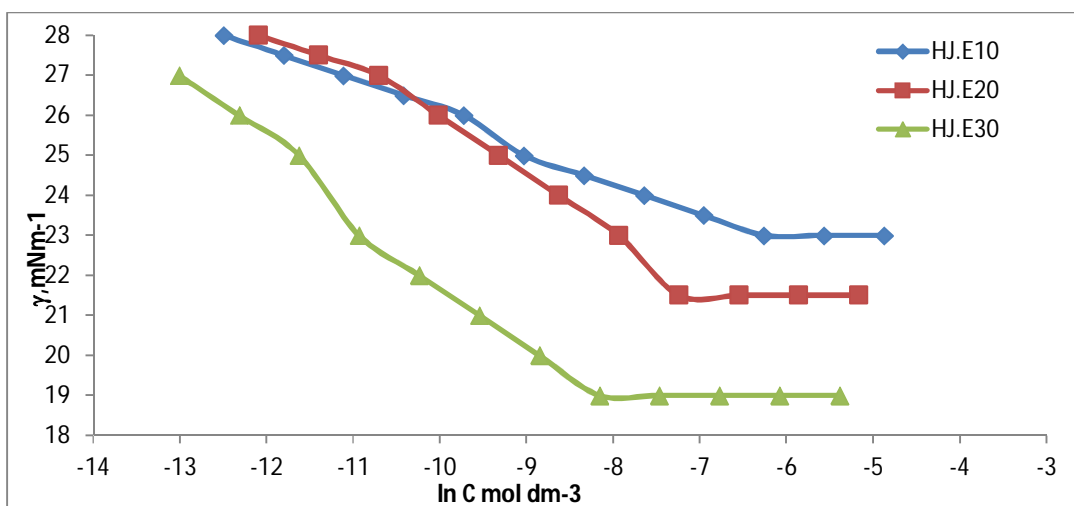


Fig. 3.8 Relationship between surface tension and $\ln C$ for ethoxylated hydrolyzed Jatropa oil at 60 °C

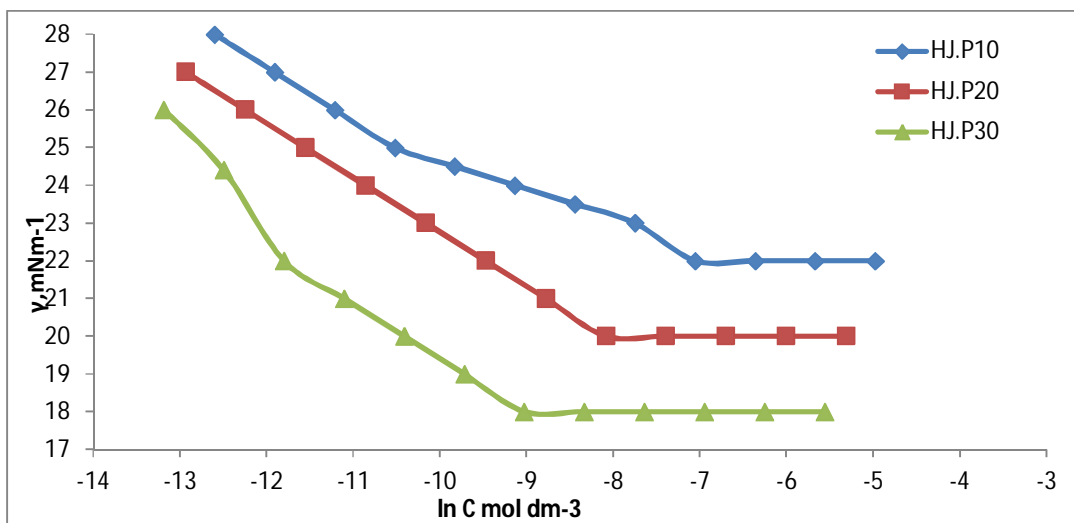


Fig. 3.9 Relationship between surface tension and $\ln C$ for propoxylated hydrolyzed Jatropa oil at 60 °C

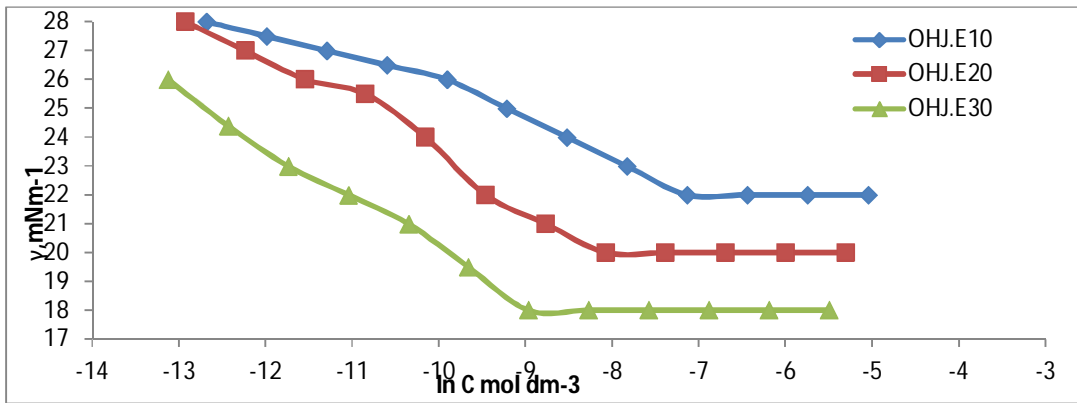


Fig. 3.10 Relationship between surface tension and ln C for oleate ethoxylated hydrolyzed Jatropha oil at 60 °C

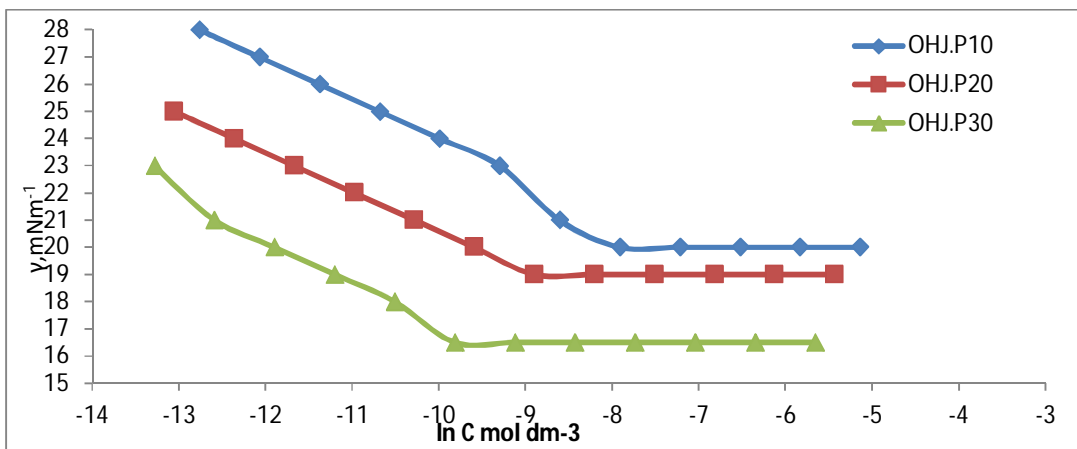


Fig. 3.11 Relationship between surface tension and ln C for oleate propoxylated hydrolyzed Jatropha oil at 60 °C

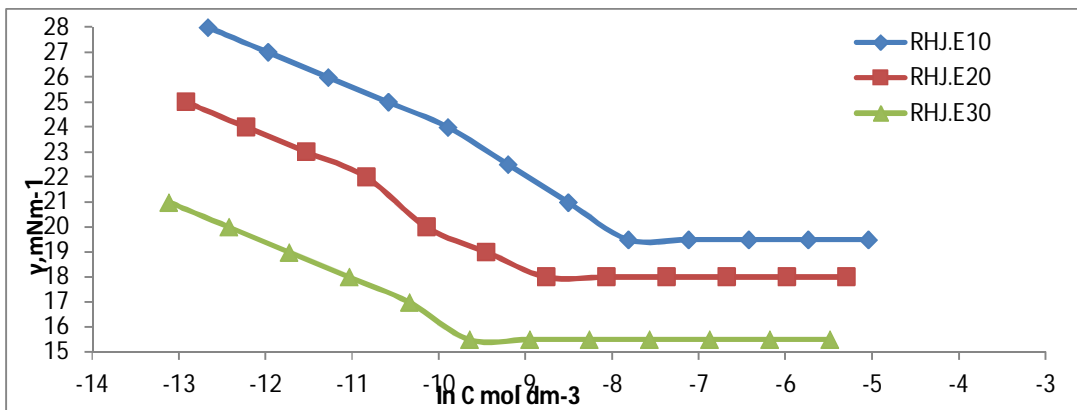


Fig. 3.12 Relationship between surface tension and ln C for rosin ethoxylated hydrolyzed Jatropha oil at 60 °C

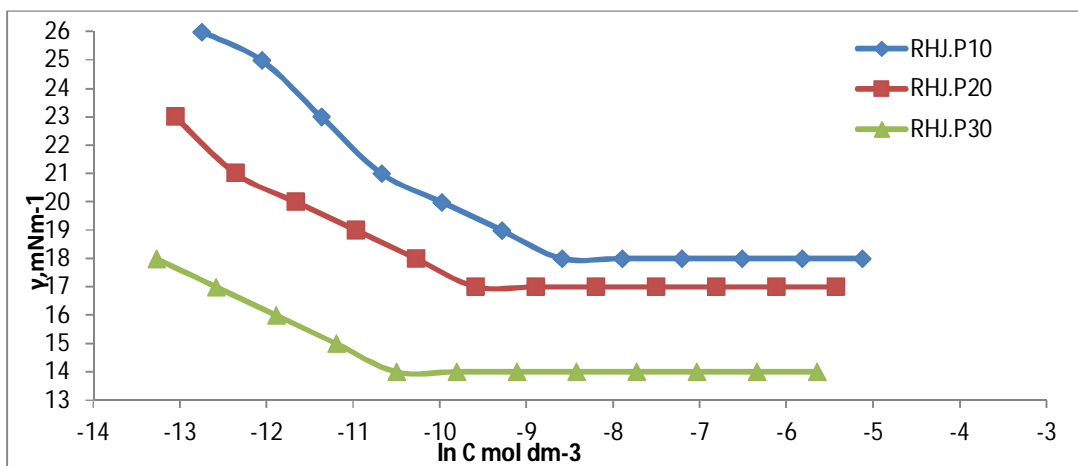


Fig. 3.13 Relationship between surface tension and lnC for rosins propoxylated hydrolyzed Jatropha oil at 60 °C

The surface tension and thermodynamic parameters of the prepared de-emulsifiers were calculated and listed in table (3.2).

It is obvious that, the CMC values decrease with increasing the temperature for all undertaken de-emulsifiers. This may be explained on the fact that, increasing the temperature leads to an increase of the mobility of the de-emulsifier that might be adsorbed on the W/O interface. It was also observed that decrease of the CMC values when the molecular weight increases. This means that the number of molecules required for micelle formation decreases as a result of the size and coiling of surfactant molecule. This finding runs in harmony with others (Tahany, 2013), they found that increasing ethylene oxide units decreases the CMC as the result of coiling the ethylene oxide chains.

Table 3.2 Surface active and thermodynamic parameters of the prepared de-emulsifiers at 60°C

De-emulsifier	Temp	CMC mole/dm ³	γ_{cmc} m N/m	$\Gamma_{max} \times 10^{-7}$ mol/m ²	A_{min} , n m ²	Π_{CMC}	ΔG_{mic} K j/mol ⁻¹	ΔG_{ads} K j/mol ⁻¹
HJ.E10	60°C	1.91x10 ⁻³	23	2.90x10 ⁻¹¹	571.85	5.0	-15.76	-17.49
HJ.E20	60°C	7.17x10 ⁻⁴	21.5	4.37x10 ⁻¹¹	379.64	6.5	-18.23	-19.72
HJ.E30	60°C	2.86 x10 ⁻⁴	19	4.44x10 ⁻¹¹	373.44	9.0	-20.55	-22.58
HJ.P10	60°C	8.67x10 ⁻⁴	22	4.13x10 ⁻¹¹	402.16	6.0	-17.75	-19.21
HJ.P20	60°C	3.10x10 ⁻⁴	20	3.92x10 ⁻¹¹	423.3	8.0	-20.35	-22.39
HJ.P30	60°C	1.20 x10 ⁻⁴	18	3.91x10 ⁻¹¹	424.1	10.0	-22.74	-25.30
OHJ.E10	60°C	8.01x10 ⁻⁴	22	4.00x10 ⁻¹¹	414.5	6.0	-17.96	-19.45
OHJ.E20	60°C	3.13x10 ⁻⁴	20	4.64x10 ⁻¹¹	357.4	8.0	-20.32	-22.05
OHJ.E30	60°C	1.28 x10 ⁻⁴	18	4.20x10 ⁻¹¹	394.5	10.0	-25.08	-26.91
OHJ.P10	60°C	3.67x10 ⁻⁴	20	4.64x10 ⁻¹¹	357.4	8.0	-21.78	-23.24
OHJ.P20	60°C	1.36x10 ⁻⁴	19	3.49x10 ⁻¹¹	475.2	9.0	-25.13	-26.77
OHJ.P30	60°C	5.5 x10 ⁻⁵	16.5	3.05x10 ⁻¹¹	543.1	11.5	-28.58	-30.68
RHJ.E10	60°C	4.10x10 ⁻⁴	19.5	4.96x10 ⁻¹¹	334.6	8.5	-21.50	-23.05
RHJ.E20	60°C	1.57x10 ⁻⁴	18	3.85x10 ⁻¹¹	431.1	10	-24.80	-26.62
RHJ.E30	60°C	6.40 x10 ⁻⁵	15.5	2.85x10 ⁻¹¹	582.5	12.5	-28.80	-31.11
RHJ.P10	60°C	1.86x10 ⁻⁴	18	4.12x10 ⁻¹¹	402.16	10	-24.2	-26.02
RHJ.P20	60°C	6.90x10 ⁻⁵	17	2.72x10 ⁻¹¹	609.6	11	-28.31	-30.31
RHJ.P30	60°C	2.75 x10 ⁻⁵	14	1.8x10 ⁻¹¹	921.26	14	-34.35	-36.91

The values of Γ_{max} and A_{min} are calculated and listed in table 3.2. It is evident that the A_{min} increases with increasing the temperature, this is probably due to the increase of thermal motion. This may be attributed to the increase of the hydrophilic moiety of ethylene oxide units in the copolymer which leads to an increase of the surface area occupied by the surfactant (de-emulsifier) molecules. It was also observed that the A_{min} was directly proportional to the molecular weight of the surfactant. The result of the thermodynamic parameters of micellization expressed by the standard Gibbs-free energy, ΔG_{mic} , (micellization) and ΔG_{ads} (adsorption), of the de-emulsifiers are listed in tables 3.2. Since ($\Delta G_{mic} < 0$), which means that the micellization is a spontaneous process, in addition, ΔG_{mic} becomes negative with the increase of the ethylene oxide units. The ΔG_{ads}

negative values are greater than ΔG_{mic} , indicating that the de-emulsifiers preferred to adsorb on the interface than to form micelles.

3.4 Effect of Hydrophilic-Lypophilic Balance (HLB)

The HLB concept is normally used as an important parameter to predict the action of de-emulsifiers on certain water- in- oil emulsion. However, this concept has not been used extensively by scientists working in the field of de-emulsifiers.

The data reveal that the amount of water separated after a certain time, expressed as percentage coalescence, is in accordance with the increase of HLB. This finding may be explained by the following speculation (Tahany, 2013).

The increase of HLB value increases the solubility of the surfactant in the aqueous phase (dispersed phase). When the de-emulsifier is initially introduced to the water-in-oil emulsion, it will be more thermodynamically stable at the interface of the water droplets. Accordingly, the concentration of the de-emulsifier in the interface increases by increasing their HLB value. As the concentration of the de-emulsifier increases at the interface, a continuous hydrophilic pathway is formed between the dispersed water droplets. This leads to rupture of the interfacial oil film surrounding the water droplets.

The present work deals with a water-in- oil emulsion, and hence it is clear that the higher the HLB, the higher the de-emulsification efficiency. The present results are consistent with this finding, as may be observed from tables 3.3, 3.4, and 3.5 for HJ.E10, 20, and 30 at concentrations of 100 and 400 ppm.

3.5 De-emulsification Efficiency

The demulsification efficiency was carried out using bottle test technique, at different five concentrations for each prepared de-emulsifier at 60 °C. The de-emulsification efficiency data for the prepared de-emulsifiers with different molecular weights in this work are shown in the tables 3.3 – 3.20. It was found that the de-emulsification efficiency increase by increasing the number of ethylene oxide units (increasing the molecular weight), HJ.E10, 20, and 30 at concentration of 100 and 400 ppm are representative example. Also HJ.E30 shoed excellent water separation compared with both HJ.E10 and HJ.E20 at all concentrations after 24 hours. But it was found that, this observation in not applicable in other concentrations, HJ.E10 exhibited good water separation at concentrations 200, 300 and 500 ppm at different time while HJ.E20 which is higher molecular weight did not.

HJ.P10, 20 and 30, showed good water separation and the separation efficiency increased with the increasing of propylene oxide units (increasing the molecular weight) for the same de-emulsifier's concentration.

OHJ.E10 showed no water separation at any concentration and any time and that can be attributed to its low HLB value (5.59), which affects the solubility of the surfactant in the aqueous phase (dispersed phase) leading to decreasing of the surfactant concentration at the interface (Zaki *et al.*, 1996) .

OHJ.E20 and OHJ.E30 showed -as expected- high efficient water separation as a result of their higher HLB values (8.73 and 10.76 respectively).

It was found that the de-emulsification efficiency increase by increasing the number of ethylene oxide units (increasing the molecular weight), OHJ.E10, OHJ.E20, and OHJ.E30 are representative example at all concentrations and at all times.

For the de-emulsifiers OHJ.P10, 20 and 30, again the molecular weight playing an important role in the water separation efficiency which is increased with increasing of the propylene oxide units for the same de-emulsifier's concentration.

RHJ.E10 showed week water separation which can be attributed to its low HLB value (5.66), while separation efficiency had higher values in RHJ.E20 and RHJ.E30 due to their higher HLB values, 8.82 and 10.84 respectively, in addition to role played by the molecular weight.

RHJ.P10, 20 and 30, showed acceptable water separation efficiency that increased with the increase of molecular weight for the same de-emulsifier concentration.

Figures (3.14-3.30) showed the water separation of the prepared de-emulsifiers at five different concentrations (Blank, 100, 200, 300, 400, and 500 ppm respectively)

The Blank sample exhibits no water separation at any time.

Table 3.3 De-emulsification efficiency of HJ.E10 at five different concentrations with time at 60°C

De-emulsifier (Effective conc. ppm)	Time / De-emulsification efficiency %				HLB	M.Wt
	60 min.	120 min.	180 min.	24 hrs.		
HJ.E10 ₍₁₀₀₎	0	0	0	0	6.72	1310
HJ.E10 ₍₂₀₀₎	25	45	45	55		
HJ.E10 ₍₃₀₀₎	45	50	55	65		
HJ.E10 ₍₄₀₀₎	0	0	0	0		
HJ.E10 ₍₅₀₀₎	30	40	45	50		



Fig. 3.14 Water separation of HJ.E10 at five different concentrations at 60°C after 24 hours

Table 3.4 De-emulsification efficiency of HJ.E20 at five different concentrations with time at 60°C

De-emulsifier (Effective conc. ppm)	Time / De-emulsification efficiency %				HLB	M.Wt
	60 min.	120 min.	180 min.	24 hrs.		
HJ.E20 ₍₁₀₀₎	5	10	25	30	10.06	1750
HJ.E20 ₍₂₀₀₎	5	5	20	20		
HJ.E20 ₍₃₀₀₎	0	0	0	10		
HJ.E20 ₍₄₀₀₎	0	0	0	10		
HJ.E20 ₍₅₀₀₎	0	0	0	20		



Fig. 3.15 Water separation of HJ.E20 at five different concentrations at 60°C after 24 hours

Table 3.5 De-emulsification efficiency of HJ.E30 at five different concentrations with time at 60°C

De-emulsifier (Effective conc. ppm)	Time / De-emulsification efficiency %				HLB	M.Wt
	60 min.	120 min.	180 min.	24 hrs.		
HJ.E30 ₍₁₀₀₎	15	45	50	55	12.05	2190
HJ.E30 ₍₂₀₀₎	40	55	75	80		
HJ.E30 ₍₃₀₀₎	40	55	75	85		
HJ.E30 ₍₄₀₀₎	15	45	50	55		
HJ.E30 ₍₅₀₀₎	5	35	50	55		



Fig. 3.16 Water separation of HJ.E30 at five different concentrations at 60°C after 24 hours

Table 3.6 De-emulsification efficiency of HJ.P10 at five different concentrations with time at 60°C

De-emulsifier (Effective conc. ppm)	Time / De-emulsification efficiency %				HLB	M.Wt
	60 min.	120 min.	180 min.	24 hrs.		
HJ.P10 ₍₁₀₀₎	10	25	50	55	0	1450
HJ.P10 ₍₂₀₀₎	20	45	45	45		
HJ.P10 ₍₃₀₀₎	5	40	40	45		
HJ.P10 ₍₄₀₀₎	10	35	35	40		
HJ.P10 ₍₅₀₀₎	0	5	10	10		



Fig. 3.17 Water separation of HJ.P10 at five different concentrations at 60°C after 24 hours

Table 3.7 De-emulsification efficiency of HJ.P20 at five different concentrations with time at 60°C

De-emulsifier (Effective conc. ppm)	Time / De-emulsification efficiency %				HLB	M.Wt
	60 min.	120 min.	180 min.	24 hrs.		
HJ.P20 ₍₁₀₀₎	20	50	50	55	0	2030
HJ.P20 ₍₂₀₀₎	35	45	60	65		
HJ.P20 ₍₃₀₀₎	30	45	45	45		
HJ.P20 ₍₄₀₀₎	20	40	40	40		
HJ.P20 ₍₅₀₀₎	0	45	45	50		



Fig. 3.18 Water separation of HJ.P20 at five different concentrations at 60°C after 24 hours

Table 3.8 De-emulsification efficiency of HJ.P30 at five different concentrations with time at 60°C

De-emulsifier (Effective conc. ppm)	Time / De-emulsification efficiency %				HLB	M.Wt
	60 min.	120 min.	180 min.	24 hrs.		
HJ.P30 ₍₁₀₀₎	45	55	55	60	0	2610
HJ.P30 ₍₂₀₀₎	55	55	60	80		
HJ.P30 ₍₃₀₀₎	45	35	55	65		
HJ.P30 ₍₄₀₀₎	25	10	40	50		
HJ.P30 ₍₅₀₀₎	45	15	65	85		



Fig. 3.19 Water separation of HJ.P30 at five different concentrations at 60°C after 24 hours

Table 3.9 De-emulsification efficiency of OHJ.E10 at five different concentrations with time at 60°C

De-emulsifier (Effective conc. ppm)	Time / De-emulsification efficiency %				HLB	M.Wt
	60 min.	120 min.	180 min.	24 hrs.		
OHJ.E10 ₍₁₀₀₎	0	0	0	0	5.59	1574.46
OHJ.E10 ₍₂₀₀₎	0	0	0	0		
OHJ.E10 ₍₃₀₀₎	0	0	0	0		
OHJ.E10 ₍₄₀₀₎	0	0	0	0		
OHJ.E10 ₍₅₀₀₎	0	0	0	0		

Table 3.10 De-emulsification efficiency of OHJ.E20 at five different concentrations with time at 60°C

De-emulsifier (Effective conc. ppm)	Time / De-emulsification efficiency %				HLB	M.Wt
	60 min.	120 min.	180 min.	24 hrs.		
OHJ.E20 ₍₁₀₀₎	15	40	60	70	8.73	2014.46
OHJ.E20 ₍₂₀₀₎	40	45	50	75		
OHJ.E20 ₍₃₀₀₎	25	35	40	50		
OHJ.E20 ₍₄₀₀₎	15	25	45	55		
OHJ.E20 ₍₅₀₀₎	20	30	45	55		



Fig. 3.20 Water separation of OHJ.E20 at five different concentrations at 60°C after 24 hours

Table 3.11 De-emulsification efficiency of OHJ.E30 at five different concentrations with time at 60°C

De-emulsifier (Effective conc. ppm)	Time / De-emulsification efficiency %				HLB	M.Wt
	60 min.	120 min.	180 min.	24 hrs.		
OHJ.E30 ₍₁₀₀₎	30	45	65	90	10.76	2454.46
OHJ.E30 ₍₂₀₀₎	35	45	50	80		
OHJ.E30 ₍₃₀₀₎	45	50	55	80		
OHJ.E30 ₍₄₀₀₎	25	50	55	80		
OHJ.E30 ₍₅₀₀₎	25	35	45	65		



Fig. 3.21 Water separation of OHJ.E30 at five different concentrations at 60°C after 24 hours

Table 3.12 De-emulsification efficiency of OHJ.P10 at five different concentrations with time at 60°C

De-emulsifier (Effective conc. ppm)	Time / De-emulsification efficiency %				HLB	M.Wt
	60 min.	120 min.	180 min.	24 hrs.		
OHJ.P10 ₍₁₀₀₎	20	30	40	50	0	1714.46
OHJ.P10 ₍₂₀₀₎	10	20	30	50		
OHJ.P10 ₍₃₀₀₎	15	25	30	45		
OHJ.P10 ₍₄₀₀₎	5	20	30	50		
OHJ.P10 ₍₅₀₀₎	0	15	30	50		



Fig. 3.22 Water separation of OHJ.P10 at five different concentrations at 60°C after 24 hours

Table 3.13 De-emulsification efficiency of OHJ.P20 at five different concentrations with time at 60°C

De-emulsifier (Effective conc. ppm)	Time / De-emulsification efficiency %				HLB	M.Wt
	60 min.	120 min.	180 min.	24 hrs.		
OHJ.P20 ₍₁₀₀₎	20	30	40	55	0	2294.46
OHJ.P20 ₍₂₀₀₎	20	30	40	50		
OHJ.P20 ₍₃₀₀₎	15	25	30	45		
OHJ.P20 ₍₄₀₀₎	10	20	35	50		
OHJ.P20 ₍₅₀₀₎	10	25	30	55		



Fig. 3.23 Water separation of OHJ.P20 at five different concentrations at 60°C after 24 hours

Table 3.14 De-emulsification efficiency of OHJ.P30 at five different concentrations with time at 60°C

De-emulsifier (Effective conc. ppm)	Time / De-emulsification efficiency %				HLB	M.Wt
	60 min.	120 min.	180 min.	24 hrs.		
OHJ.P30 ₍₁₀₀₎	25	35	45	55	0	2874.46
OHJ.P30 ₍₂₀₀₎	25	40	45	75		
OHJ.P30 ₍₃₀₀₎	40	50	50	80		
OHJ.P30 ₍₁₀₀₎	20	35	40	75		
OHJ.P30 ₍₂₀₀₎	10	25	30	55		



Fig. 3.24 Water separation of OHJ.P30 at five different concentrations at 60°C after 24 hours

Table 3.15 De-emulsification efficiency of RHJ.E10 at five different concentrations with time at 60°C

De-emulsifier (Effective conc. ppm)	Time / De-emulsification efficiency %				HLB	M.Wt
	60 min.	120 min.	180 min.	24 hrs.		
RHJ.E10 ₍₁₀₀₎	5	5	10	30	5.66	1554.43
RHJ.E10 ₍₂₀₀₎	0	0	5	25		
RHJ.E10 ₍₃₀₀₎	0	5	25	35		
RHJ.E10 ₍₄₀₀₎	0	5	20	25		
RHJ.E10 ₍₅₀₀₎	0	5	5	20		



Fig. 3.25 Water separation of RHJ.E10 at five different concentrations at 60°C after 24 hours

Table 3.16 De-emulsification efficiency of RHJ.E20 at five different concentrations with time at 60°C

De-emulsifier (Effective conc. ppm)	Time / De-emulsification efficiency %				HLB	M.Wt
	60 min.	120 min.	180 min.	24 hrs.		
RHJ.E20 ₍₁₀₀₎	10	25	30	35	8.82	1994.43
RHJ.E20 ₍₂₀₀₎	20	35	45	50		
RHJ.E20 ₍₃₀₀₎	5	25	30	40		
RHJ.E20 ₍₄₀₀₎	0	15	35	45		
RHJ.E20 ₍₅₀₀₎	20	25	30	50		



Fig. 3.26 Water separation of RHJ.E20 at five different concentrations at 60°C after 24 hours

Table 3.17 De-emulsification efficiency of RHJ.E30 at five different concentrations with time at 60°C

De-emulsifier (Effective conc. ppm)	Time / De-emulsification efficiency %				HLB	M.Wt
	60 min.	120 min.	180 min.	24 hrs.		
RHJ.E30 ₍₁₀₀₎	15	25	45	50	10.84	2434.43
RHJ.E30 ₍₂₀₀₎	20	45	50	55		
RHJ.E30 ₍₃₀₀₎	30	50	55	65		
RHJ.E30 ₍₄₀₀₎	30	50	55	75		
RHJ.E30 ₍₅₀₀₎	25	45	50	50		



Fig. 3.27 Water separation of RHJ.E30 at five different concentrations at 60°C after 24 hours

Table 3.18 De-emulsification efficiency of RHJ.P10 at five different concentrations with time at 60°C

De-emulsifier (Effective conc. ppm)	Time / De-emulsification efficiency %				HLB	M.Wt
	60 min.	120 min.	180 min.	24 hrs.		
RHJ.P10 (100)	0	10	15	25	0	1694.43
RHJ.P10 (200)	15	20	30	40		
RHJ.P10 (300)	15	20	25	50		
RHJ.P10 (400)	0	0	10	30		
RHJ.P10 (500)	0	0	0	25		



Fig. 3.28 Water separation of RHJ.P10 at five different concentrations at 60°C after 24 hours

Table 3.19 De-emulsification efficiency of RHJ.P20 at five different concentrations with time at 60°C

De-emulsifier (Effective conc. ppm)	Time / De-emulsification efficiency %				HLB	M.Wt
	60 min.	120 min.	180 min.	24 hrs.		
RHJ.P20 ₍₁₀₀₎	5	10	15	25	0	2274.43
RHJ.P20 ₍₂₀₀₎	20	30	40	50		
RHJ.P20 ₍₃₀₀₎	15	25	30	55		
RHJ.P20 ₍₄₀₀₎	10	15	25	45		
RHJ.P20 ₍₅₀₀₎	5	15	25	40		



Fig. 3.29 Water separation of RHJ.P20 at five different concentrations at 60°C after 24 hours

Table 3.20 De-emulsification efficiency of RHJ.P30 at five different concentrations with time at 60°C

De-emulsifier (Effective conc. ppm)	Time / De-emulsification efficiency %				HLB	M.Wt
	60 min.	120 min.	180 min.	24 hrs.		
RHJ.P30 ₍₁₀₀₎	10	15	25	45	0	2854.43
RHJ.P30 ₍₂₀₀₎	40	45	55	60		
RHJ.P30 ₍₃₀₀₎	25	45	50	55		
RHJ.P30 ₍₄₀₀₎	10	20	30	50		
RHJ.P30 ₍₅₀₀₎	10	15	30	50		



Fig. 3.30 Water separation of RHJ.P30 at five different concentrations at 60°C after 24 hours

3.6 Rheological behavior of the studied emulsions

It is obvious that, the yield value which is required to start the flow and the Dynamic viscosity decrease in treated emulsions.

The yield value of the dry crude oil (blank) was 2.44 D/cm² at 25 °C and it became 5.72 D/cm² for the water in oil emulsion (Water % = 20%). The increase of (τ_B) from 2.44 D/cm² for dry crude oil to 5.72 D/cm² for 20% water of the same crude oil at 25 °C, means that the presence of water droplets in the oil increases the internal pressure of the oil phase which appears during applying the shear rate as yield stress expressed as Bingham yield value. On the other hand, when the crude oil emulsion (20% water content) was treated by the de-emulsifier (OHJ.E30) at 25 °C and 400 ppm, table 3.21. The main first observation was the decrease of the (τ_B) at 25 °C up to 1.23 D/cm², the second observation was the decreasing of (τ_B) to 1.0 D/cm² by increasing of the temperature to 40°C.

By using the de-emulsifier OHJ.E30, the (τ_B) of the treated emulsion was less than the obtained for the dry crude oil and more less than the obtained (τ_B) for the crude oil emulsion (20% water content). This finding

means that the de-emulsifier molecules play a central role to decrease the viscosity of emulsion during its mobilization in the phase and the decrease of interfacial tension (surface tension) leads to enhance the water separation. Also from data in table 3.21, it was found that, the dynamic viscosities (η_{app}) was 19.8 cP for 20% W/O emulsion at 25 °C, while the dynamic viscosities (η_{app}) of the dry crude oil was 10.3 cP at 25 °C, at the same time the dynamic viscosity of the treated emulsion was 8.44 cP at 25 °C decreased to 4.16 cP when the temperature increased to 40°C.

The same results were obtained when OHJ.P30 (300ppm) and RHJ.E30 (400ppm) were studied under the same conditions, table 3.21.

Table 3.21 Rheological parameters for the freshly prepared crude oil emulsion treated with OHJ.E30 (400ppm), OHJ.P30 (300ppm) and RHJ.E30 (400ppm) at 25°C and 40°C

	Temperature	Dynamic Viscosity (cP)	Yield Value (D/cm ²)
Crude oil emulsion	25°C	19.80	5.72
Dry crude oil	25°C	10.30	2.44
Treated emulsion with OHJ.E30 (400ppm)	25°C	8.44	1.23
	40°C	4.16	1.00
Treated emulsion with OHJ.P30 (300ppm)	25°C	9.78	1.83
	40°C	4.73	0.76
Treated emulsion with RHJ.E30 (400ppm)	25°C	8.08	1.07
	40°C	4.76	0.82

3.7 Conclusion and Recommendation for further work

Certain points may be concluded and / or recommended as resulted from this study:

- (1) The de-emulsification test was carried out and the results of de-emulsification efficiency were correlated to the chemical composition of the investigated compounds. It was found that the de-emulsification efficiency increase by increasing of the number of ethylene and propylene oxide units (increasing the molecular weight).
- (2) There is a direct relationship between the HLB values and the de-emulsification efficiency, the higher the HLB, the higher the de-emulsification efficiency.
- (3) The concentration of the de-emulsifier in the interface increases by increasing their HLB value. As the concentration of the de-emulsifier increases at the interface, a continuous hydrophilic pathway is formed between the dispersed water droplets. This leads to rupture of the interfacial oil film surrounding the water droplets.
- (4) Increasing the temperature leads to decreasing of the viscosity which leads to ease the adsorption of the de-emulsifier molecules on the interface which increases the rate of water separation.
- (5) Flow properties of the emulsion with and without the de-emulsifier were investigated; the obtained results showed that, the use of de-emulsifiers enhanced the dynamic viscosity and yield value. It is obvious that, the yield value which is required to start the flow and the Dynamic viscosity decrease in treated emulsions.
- (6) ^1H -, ^{13}C -NMR and M.S. spectral analysis were recommended on order to complete the spectral properties of the prepared de-emulsifiers.

(7) Study of the prepared de-emulsifiers as possible corrosion inhibitors and viscosity depressants agents is highly recommended.